Optimal Placement of Resistive/Inductive SFCLs Considering Short-Circuit Levels Using Complex Artificial Bee Colony Algorithm

M. Esmaili [1,2*], M. Ghamsari-Yazdel [2], N. Amjady [3], C. Y. Chung [1]

1. Department of Electrical and Computer Engineering, University of Saskatchewan, Saskatoon, SK S7N 5A9 Canada.
2. Department of Electrical Engineering, West Tehran Branch, Islamic Azad University, Tehran, Iran.
3. Department of Electrical and Computer Engineering, Semnan University, Semnan, Iran.

* Corresponding author. E-mail: msdesmaili@gmail.com; m.esmaili@usask.ca.

Abstract: In mature electric power systems, growth in generation/demand, integration of renewable energy, and system expansion may elevate short-circuit levels beyond rating of existing components. Thanks to technological advancements in materials, superconducting fault current limiters (SFCLs) can effectively alleviate excessive fault currents without affecting normal operation of power systems as they are invisible in non-faulted conditions. However, due to their rather high prices, SFCL optimal placement (SOP) comes to attention. The effectiveness of SOP depends on optimally sitting of SFCL resistive/inductive types, which vary in transmission and distribution networks due to different X/R ratios. In this paper, a SOP is proposed to determine optimal locations and types of SFCLs taking into account short-circuit level of buses. In addition, a complex-valued artificial bee colony (CABC) algorithm is introduced to efficiently solve complex-valued optimization problems such as power system applications including SOP. The proposed SOP with CABC is examined on transmission and distribution test cases to evaluate its effectiveness. It is found that by employing the proposed complex decision vector (CDV), the CABC algorithm exhibits an enhanced exploration capability and convergence rate due to halving decision vector length and considering mutual effects of real and imaginary parts of decision variables.

***Index terms* — Complex artificial bee colony (CABC), complex decision vector (CDV), superconducting fault current limiter (SFCL), SFCL optimal placement (SOP), short-circuit level.**

Nomenclature

NB	Number of buses.
NG	Number of generators.
NL	Number of lines.
$\boldsymbol{Z_{mn}^{0}}$	Entry mn in the impedance matrix before installing SFCLs (pu).
$\boldsymbol{Z_{mn}^{SL}}$	SFCL impedance in series with line mn (pu).
$\boldsymbol{Z_{mn}^{PL}}$	SFCL equivalent impedance in parallel with line mn (pu).
$\Delta \boldsymbol{Z_{ij}^{mn}}$	Change in entry ij of impedance matrix due to installing SFCL on line mn (pu).
$\boldsymbol{Z_{k}^{G0}}$	Series impedance of generator k (pu).
$\boldsymbol{Z_{k}^{SG}}$	SFCL impedance in series with generator k (pu).
$\boldsymbol{Z_{k}^{PG}}$	SFCL equivalent impedance in parallel with generator k (pu).
$\Delta \boldsymbol{Z_{ij}^{k}}$	Change in entry ij of impedance matrix due to installing SFCL on generator k (pu).
$\boldsymbol{Z_{ij}^{0}}$, $\boldsymbol{Z_{ij}}$	Entry ij of impedance matrix before and after placement of SFCLs, respectively (pu).
$\boldsymbol{I_i}$	Bus i fault current after placement of SFCLs (pu).
I_i^{max}	Tolerable fault current at bus i (pu).
R_{SFCL}^{max}	Maximum allowable resistance of SFCLs (pu).
X_{SFCL}^{max}	Maximum allowable reactance of SFCLs (pu).
n_{SFCL}	Optimal number of SFCLs.
ε_R, ε_X	Threshold values for resistive/inductive SFCLs (pu).
re, im	Real and imaginary operators for complex variables.

1. Introduction

1.1. Motivation and Aims

Nowadays, fault current levels in power systems increase as a result of adding new generators and lines due to power system expansion, emerging new interactive loads in smart grids, changing from radial to meshed configurations for higher reliability, and introduction of distributed generations [1], [2]. A solution to cope with these challenges is to upgrade network components such as switchgears, circuit breakers (CBs), and cables, a measure that needs huge investments. An alternative approach is to limit fault current levels to comply with the interruption capability of components by employing superconducting fault current limiter (SFCL) technology, which is much more cost-effective than upgrading the system components. SFCLs act as invisible devices in normal operation since they exhibit a nearly zero impedance, but they present a higher impedance when activated by short-circuit currents [3], [4]. SFCLs are usually manufactured using high temperature superconducting (HTS)

components, which are immersed in a liquid nitrogen bath refrigerated by a closed-circuit loop system [5]. The highest temperature of the HTS components at the normal and at the end of fault conditions is one of key parameters in SFCL design; a typical value is 65 K and 370 K at the normal operation and at the end of faults, respectively [5].

Although SFCLs are emerging devices for future transmission and distribution systems, their installation/maintenance costs are high. In addition, their required space is an issue especially in urban areas [1]. Therefore, SFCL optimal placement (SOP) which deals with determining optimal location and size of SFCLs is becoming increasingly important [6]. This is more vital in meshed power systems, where there are various alternatives to install SFCLs. SOP can be formulated with different objective functions such as minimization of the number of SFCLs, total size of SFCLs that is proportional to total cost, protection costs, and fault current level [1].

There are three types of SFCLs including resistive (R), inductive (X), and resistive/inductive ($R + jX$) [3]. Some utilities have installed SFCLs; for example, a 9 kV/3.4 MVA resistive SFCL has been installed in 2012 as the first one in Italy [7]; a 220 kV/300 MVA inductive SFCL has been installed in 2012 in China [7]. Depending on diverse parameters including the network X/R ratios and load power factors, one type of SFCL for a candidate branch best satisfies designated objective functions. That is, a collinear SFCL may not be optimal due to different X/R ratios of branches in different locations. Therefore, a SOP problem should determine the optimal type, location, and size of SFCLs. Also, the network should be modeled with complex (resistive and inductive) impedances to accurately evaluate the effect of SFCLs on fault current levels. However, most literature works have assumed a purely resistive or inductive SFCL without considering network complex impedances.

1.2. Literature Review and Research Gaps

In [1], a SOP is proposed using an iterative technique, where one inductive SFCL is installed at each iteration, in order to evade converting the network impedance (Z_{BUS}) matrix into a variable. However, SFCL locations and sizes at previous iterations are assumed constant when the current iteration is going on. This technique may lose the optimal solution since it does not locate all SFCLs simultaneously. That is, subsequent iterations can affect optimal solutions of previous iterations. In [8], the search space of SOP is restricted by a sensitivity analysis. Although it improves solution speed, the sensitivity analysis may be valid only for a given operating point. In [6], a two-stage SOP is proposed. In the first stage, the optimal locations of SFCLs are obtained to reduce search space, whereas in the second stage, the optimal size of SFCLs is determined by a particle swarm optimization (PSO) algorithm. However, this two-stage SOP might lose the optimal solution. A SOP is proposed in [9], where the SFCL optimal locations are restricted by a sensitivity analysis and a network reduction is also used to speed up the SOP. Although short-circuit currents are modeled while installing SFCLs, the power network model is not included in the problem. In addition, sensitivity analysis and network reduction may introduce some approximations into the SOP, which is a planning problem where the execution times of methods may not be a primary concern compared to the accuracy of the solution. In [2], SFCLs are used in network reconfiguration in series with tie switches to make loops in radial distribution systems for a reduced power loss and higher reliability. The optimization problem is solved by the exhaustive search, which may be intractable in large-scale systems.

In [10], SOP is addressed to control the short-circuit level of buses in distribution systems after installing DGs by minimizing the operation times of relays and the number of SFCLs. However, neither the power network is modeled nor the impedance matrix changes caused by adding SFCLs and the short-circuit levels are considered. In [11], the optimal placement of resistive SFCLs is addressed to retain existing relay coordination when new distributed generations (DGs) are installed in a distribution system. In [12], the minimax regret criterion is used for SOP with the objective function of minimizing the impact of SFCLs on the operating times of overcurrent relays. Although these works try to optimize relay settings as before DGs, the cost of relay re-coordination is much smaller than SFCL installation cost and relay re-coordination may be done to assure efficient protection performance. Furthermore, since SFCL cost is not modeled in the problem, in some cases, preserving the original relay settings may force to employ more SFCLs leading to higher costs. In addition, location of SFCLs is determined using exhaustive search, which may be inapplicable for larger power systems. Also, a fixed size is assumed for SFCLs without obtaining their optimal sizes for each candidate branch.

In [4], resistive SFCLs in SOP are used to enhance the transient stability of a multi-machine system using the sensitivity analysis of angular separation of machines with respect to SFCL resistance. However, no optimization algorithm is presented and the model may be solvable only for small power systems. In [3], a SOP with resistive type SFCLs is addressed to optimize short-circuit currents, angular stability, and voltage stability using the PSO algorithm. In [13], an optimal power flow (OPF) is proposed where fault current levels are controlled by placement of inductive SFCLs. In [14], SOP is formulated; however, the expected values as used in the formulation may not be known before solving the problem.

In above-mentioned works, complex impedance of network branches and SFCLs are not modeled. When we place SFCLs (resistive, inductive, or resistive/inductive), we have to update the Z_{BUS} matrix after installing SFCLs to calculate fault currents. The fault currents are complex values with real and imaginary parts. In order to properly update Z_{BUS}, its updating procedure should be formulated using real and imaginary parts of Z_{BUS} and SFCL impedances.

A limited number of literature works considered complex impedances in SOP. In [15], resistive/inductive SFCL is optimally placed using a PSO algorithm. However, the updating procedure of Z_{BUS} is not formulated. Also, the number of control variables of the PSO algorithm is doubled as resistive and inductive parts of SFCLs are considered; this feature may limit the tractability of the method in large-scale systems. Moreover, the number of SFCLs is not optimized, an uneconomical feature that might result in placing SFCLs on almost all branches.

In fact, if we aim to formulate SOP as a mixed-integer nonlinear programming (MINLP) problem to update the Z_{BUS} ma-

trix with complex impedances of branches and SFCLs, the optimization constraints turn into highly nonlinear/nonconvex terms. It happens due to modeling the effect of SFCLs with complex-valued impedances on the network. Because of a high level of nonlinearity/nonconvexity, the MINLP problem of SOP may become intractable even for small power systems. On the other hand, evolutionary algorithms, which are usually programmed with MATLAB scripts, exhibit good performance in handling such problems due to built-in functions of MATLAB for complex numbers. Out of the evolutionary algorithms, the artificial bee colony (ABC) is easy to implement, flexible, and robust against initialization. It also needs fewer control parameters and works well with discrete variables [16]. It offers an effective search process for highly complex problems with a low risk of premature convergence [17]. The ABC is previously applied to power system applications [18], [19]. Thus, an enhanced version of ABC with the ability of processing complex variables, i.e. the complex ABC (CABC) algorithm, is presented in this research work to solve the proposed SOP problem, which is highly nonlinear/nonconvex, includes discrete variables, and is sensitive to initialization.

When evolutionary algorithms are applied to power system applications where we have n complex decision variables (such as $R + jX$ of SFCLs in SOP), the decision vector is assumed a $2n$-sized vector containing R and X of SFCLs [15]. Although this technique models resistive/inductive SFCLs, it assumes no connection between R and X parts of individual SFCLs. Alternatively, we here present the concept of complex decision vector (CDV) which is more efficient and faster in approaching the final solution for complex optimization problems such as power system applications. In the CDV, we assume a decision vector with n *complex* entries; for instance, in the SOP problem, it contains SFCL complex sizes as $R + jX$. The CDV not only halves the length of decision vector implying a faster convergence, but also it improves the exploration capability of evolutionary algorithms due to considering interactive effects of real and imaginary parts of decision variables. A comprehensive comparison will be presented in Section 4 of this paper. It is noted that although we implement CDV in this paper with ABC, the CDV concept can easily be applied to other evolutionary algorithms.

1.3. Contributions and Organization of the Paper

In light of literature review, the main contributions of this paper can be summarized as:

- An SOP model is proposed to determine the optimal type, location, and size of SFCLs. An optimization method is also presented to minimize the number and size of resistive/inductive SFCLs.
- The concept of CDV is proposed for the ABC algorithm leading to a new complex ABC (CABC) method. The proposed CABC offers higher exploration capability and solution speed in solving the complex-valued SOP problem.
- A modified procedure is presented to accurately calculate fault currents after installing resistive/inductive SFCLs considering real and imaginary parts of SFCL, Z_{BUS} impedances, and fault currents. The proposed approach can be applied to meshed/radial distribution and transmission networks. Moreover, it is possible to set a different limit for fault current of each line in order to enhance transient stability and reliability of vulnerable branches.

The rest of this paper is organized as follows. In Section 2, the proposed model for SOP is explained. In Section 3, the CABC algorithm is introduced to solve the proposed SOP problem. Section 4 delineates case study results and discussions. Finally, Section 5 concludes the paper.

2. Proposed SOP Model

2.1. Effect of SFCL placement on network impedance matrix

The effect of an activated SFCL impedance $\boldsymbol{Z_{mn}^{SL}}$ in series with line mn impedance is equal to inserting impedance $\boldsymbol{Z_{mn}^{PL}}$ in parallel with line mn impedance [8] (we denote complex numbers in this paper with bold fonts):

$$\boldsymbol{Z_{mn}^{PL}} = -\frac{\boldsymbol{Z_{mn}^{0}}(\boldsymbol{Z_{mn}^{0}} + \boldsymbol{Z_{mn}^{SL}})}{\boldsymbol{Z_{mn}^{SL}}} \,. \tag{1}$$

The effect of inserting the SFCL equivalent parallel impedance on impedance matrix entry ij is reflected as [8]:

$$\Delta \boldsymbol{Z_{ij}^{mn}} = -\frac{(\boldsymbol{Z_{im}^{0}} - \boldsymbol{Z_{in}^{0}})(\boldsymbol{Z_{mj}^{0}} - \boldsymbol{Z_{nj}^{0}})}{\boldsymbol{Z_{mm}^{0}} + \boldsymbol{Z_{nn}^{0}} - 2\boldsymbol{Z_{mn}^{0}} + \boldsymbol{Z_{mn}^{PL}}} \,. \tag{2}$$

Since SFCLs are not installed on all branches (i.e., $\boldsymbol{Z_{mn}^{SL}} = 0$), we obtain $\boldsymbol{Z_{mn}^{PL}} = \infty$ from (1) for branches without SFCLs. This situation generates a division-by-zero error in calculations when handling (1). Therefore, we omit $\boldsymbol{Z_{mn}^{PL}}$ from equations by substituting (1) in (2):

$$\Delta \boldsymbol{Z_{ij}^{mn}} = -\frac{\boldsymbol{Z_{mn}^{SL}}(\boldsymbol{Z_{im}^{0}} - \boldsymbol{Z_{in}^{0}})(\boldsymbol{Z_{mj}^{0}} - \boldsymbol{Z_{nj}^{0}})}{\boldsymbol{Z_{mn}^{SL}}(\boldsymbol{Z_{mm}^{0}} + \boldsymbol{Z_{nn}^{0}} - 2\boldsymbol{Z_{mn}^{0}}) - \boldsymbol{Z_{mn}^{0}}(\boldsymbol{Z_{mn}^{0}} + \boldsymbol{Z_{mn}^{SL}})} \,. \tag{3}$$

Equation (3) gives a compact expression for the change in Z_{BUS} complex entries considering the SFCL series impedance $\boldsymbol{Z_{mn}^{SL}}$ on line mn.

Similarly, the effect of inserting SFCL impedance $\boldsymbol{Z_{k}^{SG}}$ in series with existing generator impedance $\boldsymbol{Z_{k}^{G0}}$ is equal to inserting impedance $\boldsymbol{Z_{k}^{PG}}$ in parallel with $\boldsymbol{Z_{k}^{G0}}$ [20]:

$$\boldsymbol{Z_{k}^{PG}} = -\frac{\boldsymbol{Z_{k}^{G0}}(\boldsymbol{Z_{k}^{G0}} + \boldsymbol{Z_{k}^{SG}})}{\boldsymbol{Z_{k}^{SG}}} \,. \tag{4}$$

The change in Z_{BUS} complex entries due to $\boldsymbol{Z_{k}^{PG}}$ is given as [20]:

$$\Delta \boldsymbol{Z_{ij}^{k}} = -\frac{\boldsymbol{Z_{ik}^{0}} \cdot \boldsymbol{Z_{kj}^{0}}}{\boldsymbol{Z_{kk}^{0}} + \boldsymbol{Z_{k}^{PG}}} \,. \tag{5}$$

By substituting (4) in (5) to omit $\boldsymbol{Z_{k}^{PG}}$ (to avoid division-by-zero error), the change in Z_{BUS} entries considering generator SFCL series impedance $\boldsymbol{Z_{k}^{SG}}$ is given as:

$$\Delta \boldsymbol{Z_{ij}^{k}} = -\frac{\boldsymbol{Z_{ik}^{0}} \cdot \boldsymbol{Z_{kj}^{0}} \cdot \boldsymbol{Z_{k}^{SG}}}{\boldsymbol{Z_{kk}^{0}} \cdot \boldsymbol{Z_{k}^{SG}} - \boldsymbol{Z_{k}^{G0}}(\boldsymbol{Z_{k}^{G0}} + \boldsymbol{Z_{k}^{SG}})} \,. \tag{6}$$

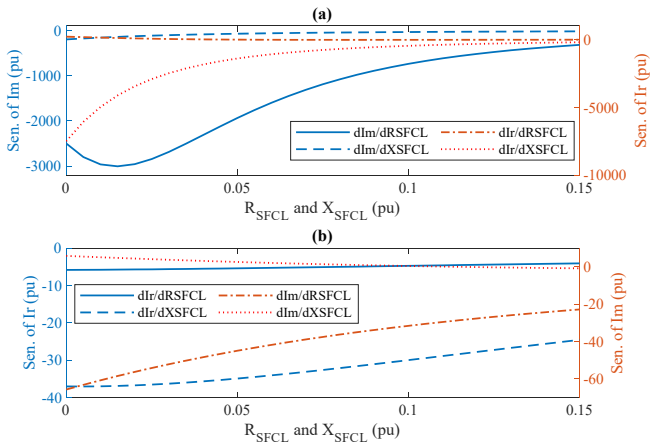

Fig. 1. *Sensitivity of imaginary and real parts of bus fault currents with respect to resistive and inductive SFCL,* ***(a):*** *a transmission system,* ***(b):*** *a distribution system.*

2.2. Objective functions and constraints

Objective functions of the proposed SOP model include minimization of the number of SFCLs and their total impedances (which are proportional to their total cost):

$$\min\ F_1 = num\left(\sum_{n=1}^{NB}\sum_{m=n+1}^{NB} \boldsymbol{Z_{mn}^{SL}} + \sum_{k=1}^{NG} \boldsymbol{Z_k^{SG}}\right), \tag{7}$$

$$\min\ F_2 = abs\left(\sum_{n=1}^{NB}\sum_{m=n+1}^{NB} \boldsymbol{Z_{mn}^{SL}} + \sum_{k=1}^{NG} \boldsymbol{Z_k^{SG}}\right), \tag{8}$$

where operators abs and num indicate the number of SFCLs and the magnitude of complex numbers, respectively. In (8), the abs operator is applied to the complex-valued summation of SFCL impedances. Decision variables of the optimization problem consist of SFCLs installed on lines ($\boldsymbol{Z_{mn}^{SL}}$) and generators ($\boldsymbol{Z_k^{SG}}$). It should be noted that without considering the first objective function, the problem may place small SFCLs on almost all buses, a result that is unfavorable.

After placement of SFCLs in series with lines and generators, entries of Z_{BUS} are updated as formulated by (1)–(6). Since we are interested in diagonal entries of Z_{BUS} to calculate bus fault currents, they are updated as:

$$\boldsymbol{Z_{ii}} = \boldsymbol{Z_{ii}^0} + \sum_{n=1}^{NB}\sum_{m=1}^{NB} \Delta \boldsymbol{Z_{ii}^{mn}} + \sum_{k=1}^{NG} \Delta \boldsymbol{Z_{ii}^{k}}\ , \tag{9}$$

where $\Delta \boldsymbol{Z_{ii}^{mn}}$ and $\Delta \boldsymbol{Z_{ii}^{k}}$ are specified by (3) and (6), respectively. Bus fault currents are calculated from diagonal entries of the updated impedance matrix:

$$\boldsymbol{I_i} = 1/\boldsymbol{Z_{ii}}. \tag{10}$$

Bus fault currents should be limited to their tolerable short-circuit levels (this goal is achieved by placement of optimal SFCLs):

$$abs(\boldsymbol{I_i}) \le I_i^{max}. \tag{11}$$

The resistive and inductive impedances of SFCLs should be limited to their allowable ranges:

$$\varepsilon_R \le re(\boldsymbol{Z_{mn}^{SL}}) \le R_{SFCL}^{max}\ ,\ \ \varepsilon_X \le im(\boldsymbol{Z_{mn}^{SL}}) \le X_{SFCL}^{max}. \tag{12}$$

$$\varepsilon_R \le re(\boldsymbol{Z_k^{SG}}) \le R_{SFCL}^{max}\ ,\ \varepsilon_X \le im(\boldsymbol{Z_k^{SG}}) \le X_{SFCL}^{max}. \tag{13}$$

In order to numerically stabilize the problem convergence while numerating the number of SFCLs in (7), only values that are greater than threshold ε_R or ε_X are counted as constrained by (12)–(13). The threshold is chosen a small value so that it does not affect calculations (10^{-4} pu in our simulations).

2.3. Sensitivity of bus fault current with respect to SFCL

Consider the Thevenin equivalent of a network at the installation point of SFCL having impedance $\boldsymbol{Z_{SFCL}} = R_{SFCL} + jX_{SFCL}$. The equivalent circuit before placing SFCL is obtained as a voltage source in series with $\boldsymbol{Z_{ii}} = R_{ii} + jX_{ii}$. Therefore, the equivalent circuit with SFCL is composed of a voltage source in series with $\boldsymbol{Z} = \boldsymbol{Z_{ii}} + \boldsymbol{Z_{SFCL}} = R + jX = (R_{ii} + R_{SFCL}) + j(X_{ii} + X_{SFCL})$. Without loss of generality, we assume the voltage source of Thevenin equivalent as 1 pu. Therefore, the fault current can be expressed as:

$$I = \frac{1}{R + jX} = \frac{R}{R^2 + X^2} - j\frac{X}{R^2 + X^2}\ . \tag{14}$$

Thus, the absolute value of real and imaginary parts of the fault current is obtained as $I_{re} = R/(R^2 + X^2)$ and $I_{im} = X/(R^2 + X^2)$. The sensitivities of these currents with respect to R_{SFCL} and X_{SFCL} can be obtained as:

$$\frac{\partial I_{re}}{\partial R_{SFCL}} = \frac{X^2 - R^2}{(R^2 + X^2)^2}\quad ,\quad \frac{\partial I_{re}}{\partial X_{SFCL}} = \frac{-2X}{(R^2 + X^2)^2}\ . \tag{15}$$

$$\frac{\partial I_{im}}{\partial R_{SFCL}} = \frac{-2R}{(R^2 + X^2)^2}\quad ,\quad \frac{\partial I_{im}}{\partial X_{SFCL}} = \frac{R^2 - X^2}{(R^2 + X^2)^2}\ . \tag{16}$$

In view of the fact that R and X are total values including R_{SFCL} and X_{SFCL}, the sensitivities in (15)-(16) are functions of SFCL impedances. In order to visualize the effect of SFCL resistive and inductive parts on the sensitivities, they are plotted in Fig. 1. In transmission-level power systems, fault currents may have mostly imaginary parts, whereas they may have considerable real parts in distribution system. In Fig. 1(a), the variation of $\partial I_{im}/\partial R_{SFCL}$ is plotted versus R_{SFCL} and $\partial I_{im}/\partial X_{SFCL}$ is plotted versus X_{SFCL}. Both curves represent negative values implying that imaginary fault current decrease by installing SFCLs. As seen, the imaginary fault current exhibits higher sensitivity to resistive SFCL in transmission systems. That is, a mostly resistive SFCL reduces I_{im} better than an inductive SFCL. The sensitivities of the real parts are also depicted in Fig. 1(a). However, since the magnitudes of the real parts of fault currents may be small in transmission systems, they may not affect the system behavior even though they present higher sensitivities. In Fig. 1(b), the real part of fault current is represented in a distribution test system and the variation of $\partial I_{re}/\partial R_{SFCL}$ is plotted versus R_{SFCL} and $\partial I_{re}/\partial X_{SFCL}$

is plotted versus X_{SFCL}. As seen, the real part of fault current has higher sensitivity with respect to inductive SFCL in all ranges of SFCL reactance. As a result, an inductive SFCL can better mitigate fault currents in a distribution system. The sensitivities of the imaginary parts of fault currents are also depicted in Fig. 1(b). However, since the imaginary parts may have a lower magnitude in distribution systems, they may less affect the system behavior even though they present a high sensitivity.

2.4. Multi-objective solution approach

We assume the number of SFCLs in (7) as the main objective function. We employ a lexicographic optimization method for multi-objective optimization [21]. In the first stage, F_1 in (7) is individually minimized (without minimizing F_2). The result that is obtained from this stage represents the best attainable number of SFCLs: we call it n_{SFCL}. In the second stage, the second objective function (8) is minimized as:

$$\text{Min } F_2 \tag{17}$$

s.t.

$$F_1 \leq n_{SFCL}. \tag{18}$$

$$(3), (6)\text{–}(13). \tag{19}$$

This approach ensures the best value for the first objective function while it also optimizes the second objective function.

3. Complex ABC (CABC) as the Solution Approach

In this section, the basic ABC algorithm is first reviewed briefly and then, the proposed CABC method is introduced.

3.1. Basic Artificial Bee Colony (ABC) algorithm

The ABC algorithm has been previously employed in power system applications such as in [18], [19]. In ABC, there are three types of bees: employed, onlooker, and scout. An employed bee goes to a previously discovered food position (solution) area and evaluates its neighborhood nectars. If the nectar of a new food position is higher than the previous one, the employed bee memorizes it and forgets the previous one. Employed bees share their information by dancing in the hive. By watching the dance, onlooker bees choose higher quality food positions (i.e., lower cost solutions) from those exploited by employed bees. Scout bees are translated from a few employed bees who abandon their food position and search for new ones.

The first and second half of the bee colony consist of employed and onlooker bees, respectively. The number of solutions is equal to the number of employed or onlooker bees. Let $X_{i,t}$ represent candidate solution vector i at iteration t. The pseudo-code of ABC algorithm is as follows:

1. For each solution vector i, generate initial position randomly considering lower and upper bounds of decision variables.
2. For all iterations, do:
3. Loop over employed bees:
   a. Calculate new positions: $X_{i,t+1} = X_{i,t} + \phi(X_{i,t} - X_{j,t})$ where $\phi = a.r$; $X_{j,t}$ is a randomly selected solution ($j \neq i$); a is the acceleration factor and r is a random number uniformly generated in interval [−1,1].
   b. Bound new positions to decision variables' limits.
   c. Evaluate cost of old and new positions. For each solution vector i, if new position $X_{i,t+1}$ has a better cost than old position $X_{i,t}$, replace $X_{i,t}$ by $X_{i,t+1}$.
   d. Calculate probabilities for roulette wheel selection approach: $P_i = F_i / \sum_{j=1}^{n} F_j$, where $F_i = e^{-C_i}/\overline{C}$ translates cost to fitness; P_i is the probability of selection of solution i; F_i is the fitness of solution i; C_i is the cost of solution i: the cost objective function C_i can be the number of SFCLs in (7) or total impedance of SFCLs in (8); $\overline{C}$ is the mean cost of solutions.
4. Loop over onlooker bees:
   a. Select the best food source (say i) using probabilities.
   b. Calculate new positions: $X_{i,t+1} = X_{i,t} + \phi(X_{i,t} - X_{j,t})$ where $\phi = a.r$; $X_{j,t}$ is a randomly selected solution ($j \neq i$); a is the acceleration factor and r is a random number uniformly generated in interval [−1,1].
   c. Bound new positions to decision variables' limits.
   d. For each solution vector i, if new position $X_{i,t+1}$ has a lower cost than old position $X_{i,t}$, replace $X_{i,t}$ by $X_{i,t+1}$.
5. Scout bees: if a solution stagnation time exceeds the abandonment limit, replace its position with a randomly generated position.
6. Update the best solution ever found.
7. If the convergence criterion is met, stop and return the best solution; otherwise go to step 2.

3.2. Proposed Complex ABC (CABC) algorithm

When there are n-dimensional complex decision variables in a complex-valued application, such as phasor calculations in power systems, literature works separate real and imaginary parts of decision variables and constitute a $2n$-dimensional decision vector to be optimized by evolutionary algorithms. This process not only may be intractable in large-scale applications (due to doubled length of the decision vector), but also ignores the coupling of real and imaginary parts of decision variables.

In developing CABC, we consider complex decision variables to constitute CDV. Without loss of generality, we presume the complex impedance of SFCLs as decision variables: $\boldsymbol{Z_l^{SL}} = R_l^{SL} + jX_l^{SL}$ (l is the index of lines) and $\boldsymbol{Z_k^{SG}} = R_k^{SG} + jX_k^{SG}$ (k is the index of generators). Then, the CDV becomes:

$$\boldsymbol{X} = \begin{bmatrix} R_1^{SL} + jX_1^{SL} \\ R_2^{SL} + jX_2^{SL} \\ \vdots \\ R_{NL}^{SL} + jX_{NL}^{SL} \\ R_1^{SG} + jX_1^{SG} \\ R_2^{SG} + jX_2^{SG} \\ \vdots \\ R_{NG}^{SG} + jX_{NG}^{SG} \end{bmatrix}. \tag{20}$$

Based on this decision vector, the following modifications are applied to basic ABC to derive the proposed CABC:

- Initial position for each candidate solution is generated as complex numbers: $\boldsymbol{X_{i,1}} = f_{ur}(i) + jg_{ur}(i)$ where $f_{ur}(i)$ and $g_{ur}(i)$ are random number generators with uniform distribution in the decision variables' limits for bee i.
- New positions are updated as: $\boldsymbol{X_{i,t+1}} = \boldsymbol{X_{i,t}} + \phi(\boldsymbol{X_{i,t}} - \boldsymbol{X_{j,t}})$ as complex vectors.
- New complex positions are bounded to decision variables' limits:

$$\boldsymbol{X_{i,t+1}} = \max(re(\boldsymbol{X_{i,t+1}}), \alpha_i^{min}) + j\max\left(im(\boldsymbol{X_{i,t+1}}), \beta_i^{min}\right), \tag{21}$$

$$\boldsymbol{X_{i,t+1}} = \min(re(\boldsymbol{X_{i,t+1}}), \alpha_i^{max}) + j\min\left(im(\boldsymbol{X_{i,t+1}}), \beta_i^{max}\right), \tag{22}$$

  where α_i^{min} and α_i^{max} are allowable limits for real part of decision variable i; β_i^{min} and β_i^{max} are allowable limits for imaginary part of decision variable i. The first and second terms in (21) set the real and imaginary parts of new position, respectively, to their lower bounds if they violate the lower limits. Similarly, (22) imposes the upper limits.
- Scout bees: stagnated positions are replaced with new complex positions that are uniformly generated respecting decision variable limits: $\boldsymbol{X_{i,1}} = f_{ur}(i) + jg_{ur}(i)$.
- In evaluating the cost of positions, calculations (updating of impedance matrix and bus fault currents) are done using complex numbers.

By employing CDV in the CABC algorithm, we retain the coupling of real and imaginary parts of decision variables to obtain a faster convergence and higher quality solution.

4. Case Studies and Numerical Experiments

4.1. Evaluating the proposed multi-objective solution method on standard benchmark functions

Prior to presenting the results of the proposed method on the examined power system test cases, we evaluate its effectiveness by comparing its results with the results of some other multi-objective solution methods on two standard benchmark multi-objective problems. These two problems, called here P1 and P2, are as follows [22]:

$$\text{Problem P1: } \min\ (f_1, f_2) \tag{23}$$

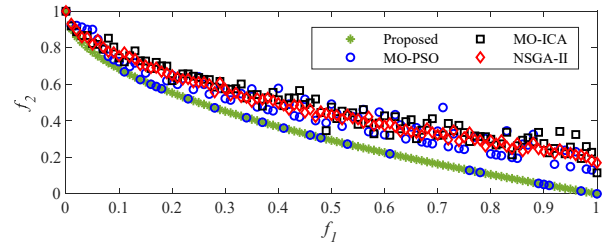

Fig. 2. *Non-dominated fronts of the first benchmark problem obtained by examined methods.*

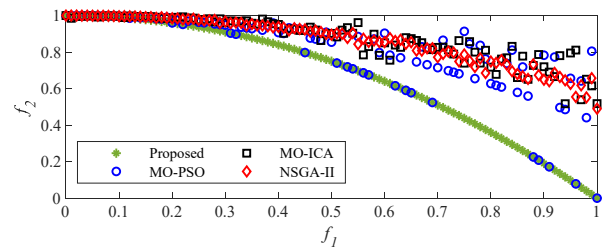

Fig. 3. *Non-dominated fronts of the second benchmark problem obtained by examined methods.*

$$\text{s.t.} \quad f_1(x_1) = x_1\ , \tag{24}$$

$$g(x_2, x_3, \dots, x_m) = 1 + 9\sum_{i=2}^{m}\{x_i/(m-1)\}\ , \tag{25}$$

$$f_2(f_1, g) = 1 - \sqrt{f_1/g}. \tag{26}$$

$$\text{Problem P2: } \min\ (f_1, f_2) \tag{27}$$

$$\text{s.t. (24)-(25)}, \tag{28}$$

$$f_2(f_1, g) = 1 - (f_1/g)^2. \tag{29}$$

where $m = 30$, $x_i \in [0,1]$. In fact, P1 and P2 have a convex and concave optimal Pareto fonts, respectively [22].

To evaluate the effectiveness of our proposed multi-objective method (comprising CABC and lexicographic optimization), we compare it with multi-objective PSO (MO-PSO), multi-objective imperialist competitive algorithm (MO-ICA), and non-dominated sorting genetic algorithm-II (NSGA-II). The results of running the proposed method and the three comparative methods on the two mentioned benchmark optimization problems of P1 and P2 are shown in Fig. 2 and Fig. 3, respectively. To have a fair comparison, the maximum number of iterations and the population size are considered as 100 and 50, respectively, for all examined methods.

As seen from Fig. 2 and Fig. 3, the proposed method is able to obtain a more optimal Pareto front compared to other methods. The MO-PSO method is able to catch the Pareto-front as good as the proposed method only at some values of objective functions. In the next position, NSGA-II stands and the MO-ICA method stands at the last position.

4.2. Assumptions

In order to evaluate the performance and robustness of the proposed methodology in both transmission and distribution systems, it is examined on the IEEE test systems including the 30-bus transmission test system [23] and the 31-bus distribution

test system [24]. All simulations are carried out in MATLAB software environment on a 2.6 GHz Intel Core i5 laptop computer with 4 GB RAM. In the transmission test system, it is assumed that short-circuit levels exceed the allowable rating of switchgears and CBs (40 kA) as a result of system expansion including installation of new generation units and parallel branches. In the distribution 31-bus test system, it is supposed that fault current levels exceed the allowable rating of switchgears and CBs (12.5kA) as a result of adding a few DG units. Therefore, SFCLs are required to mitigate fault current levels in both test systems. Here, we consider 3-phase faults as the worst case in the SOP problem. Note that since power system short-circuit study is usually performed at the worst case (e.g., all generators and lines are connected), there is no need to consider safety margins for short-circuit levels. The CABC parameters including colony size, number of onlooker bees, and the abandonment limit are considered 50, 50, and 1410, respectively by try and error.

In order to include economic aspects of SFCLs, capital (installation) and device costs of SFCLs should be considered. The cost details are presented in Table 1 according to nominal voltages of SFCLs. Capital costs are adopted from [1]. For the device cost of SFCLs, we use the data provided by the SuperOx company [25] as one of SFCL manufacturers. In the last column of this table, the device cost of SFCL is reported in terms of its normalized value per impedance of SFCLs. We use these values in our simulations in the next subsections.

4.3. IEEE 30-bus transmission test system

In Fig. 4, bus fault current levels before SOP are shown for the IEEE 30-bus case study, the one-line diagram of which is depicted in Fig. 5. Fault currents in Fig. 4 are given in real and imaginary parts with their absolute values as well as their allowable limit (40kA). As seen, the absolute value of fault current (as shown by blue bars) exceeds its allowable limit at six buses. The highest fault current occurs at bus 2 with 60.37 kA. Therefore, to achieve a cost-effective SOP solution, it is required to place the optimal value of the proper SFCL type at optimal locations. As seen in Fig. 4, imaginary parts of fault currents dominate their real parts due to a high X/R ratio in transmission systems.

The optimal locations, sizes, and types of SFCLs are reported in Table 2. As seen in Fig. 5, the proposed SOP installs 3 generator SFCLs at buses 1, 2, and 22 without branch SFCLs. This result is reasonable as generator SFCLs may better mitigate fault currents since generators serve as sources of fault currents. According to Table 2, generator SFCL at bus 1 is mostly inductive, while it is purely resistive at bus 2. For bus 3, it is mostly resistive. The total SFCL impedance in Table 2 is 7.8554 + j2.027 Ω, which is mostly resistive. This happens because the fault currents in this transmission test system exhibit a higher sensitivity to resistive SFCL than inductive one due to their dominant imaginary component (see Fig. 4). As discussed in Subsection 2.3, the imaginary fault current exhibits a higher sensitivity with respect to a resistive SFCL. In addition, a resistive SFCL moderates the high X/R ratios in this transmission system. In addition, the SOP optimization problem employs

Table 1. Cost details of SFCLs.

Voltage level (kV)	Capital cost [1] (M$)	Typical rated power [25] (MW)	Typical impedance [25] (Ω)	Device cost (M$/Ω)
0.4	0.5	5	0.5	1.00
6	0.5	20	1	1.60
20	0.5	30	8	0.30
110	1	200	25	0.48
220	1.5	500	50	0.60

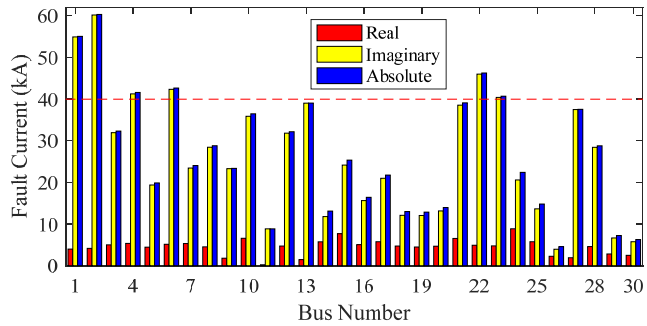

Fig. 4. *Bus fault currents of IEEE 30-bus transmission test system before SOP.*

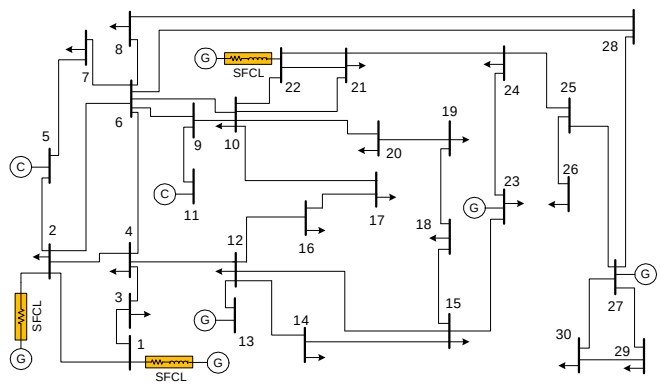

Fig. 5. *One-line diagram of the IEEE 30-bus transmission test system.*

Table 2. Optimal location and size of SFCLs in the IEEE 30-bus transmission test system obtained by the proposed SOP

Location	SFCL impedance (Ω)
Gen. at bus 1	0.5873 + j1.2143
Gen. at bus 2	4.6011 + j0
Gen. at bus 22	2.6670 + j0.8127
Total	**7.8554 + j2.027**

some inductive SFCLs to satisfy the objective function and obtain lower fault current levels. In this case study, since a resistive SFCL is installed at bus 2 and this bus is connected to bus 1 (see Fig. 5), the major part of bus 1 and 2 imaginary fault currents is alleviated by the resistive SFCL at bus 1. Therefore, the optimization problem installs some inductive SFCL at bus 1 to further limit fault currents and keep the objective function under control at the same time.

Bus fault currents after installing SFCLs are depicted in Fig. 6. As seen, the absolute values of all fault currents (the blue

bars) are limited to the allowable limit of 40kA in Fig. 6.

In order to analyze variation of fault currents after placing SFCLs, we here define the index of total imaginary to real (TIR) for bus fault currents as: $TIR = \sum_{i=1}^{NB}\{im(\boldsymbol{I_i})\} / \sum_{i=1}^{NB}\{re(\boldsymbol{I_i})\}$. A higher TIR implies the higher dominance of imaginary part of fault currents with respect to their real part on average. The value of TIR index decreases from 5.84 in Fig. 4 to 3.52 in Fig. 6. This result indicates that the SOP has decreased imaginary parts of fault current more than their real parts by placing proper types of SFCLs. The proposed SOP is able to adjust real and imaginary parts of fault currents since it can select proper type and value of SFCLs. As a result, the proposed SOP limits fault currents by the least possible SFCL sizes compared with the literature works.

In Table 3, the results of the proposed SOP using the original ABC and the proposed CABC algorithms are compared with the results of some literature woks on the IEEE 30-bus test system. It is noted that each article has its own assumptions such as allowable short-circuit level and network impedances in the case studies. Thus, it may not be possible to simply compare the results of different SOP works in a fair manner. To overcome this problem, we establish a fair framework in Table 3 to compare SOP results. In the second row of this table, the total amount of excessive fault currents is given for all methods. For instance, for the proposed SOP method, it represents summation of fault currents (absolute value of sum of complex currents) beyond the 40 kA allowable limit in Fig. 4. That is, we have 46.790 kA excessive fault currents in our test case that should be alleviated by SFCLs. The second row of Table 3 shows that our proposed SOP encounters a higher excessive fault current value than the other methods on the same test system. Thus, the proposed SOP should solve a more complex test case than the other methods. In rows 3 and 4 of Table 3, the optimal number and size of SFCLs obtained by the SOP methods are given, respectively. It is seen that the proposed SOP with the CABC algorithm results in lower total SFCL size than the other methods. Taking into account this fact that the size of SFCL is a measure of its cost, a lower total SFCL size implies a more cost-effective solution. This better performance of the proposed SOP should be considered along with its more complex test case, which further illustrates higher effectiveness of the proposed SOP than the other methods of Table 3. Indeed, the proposed SOP with the CABC algorithm only needs 8.113 Ω SFCL (which is the lowest in Table 3) to mitigate excessive fault current 46.790 kA (which is the highest in Table 3). To better illustrate higher effectiveness of the proposed SOP, the index of average SFCL impedance per fault current (ASIPFC) is calculated and reported in row 5 of Table 3. For example, method [8] needs 42.471Ω SFCL to alleviate 16.551kA excessive fault currents, which results in ASIPFC = 42.471Ω /16.551kA = 2.566 Ω/kA. That is, this method needs 2.566Ω SFCL to mitigate one kA of fault current. The ASIPFC index can be considered as the efficiency of SFCL placement methods in consuming the SFCL resource to mitigate excessive fault currents. As seen in Table 3, the proposed SOP with the CABC algorithm leads to ASIPFC = 0.173 Ω/kA, which is much better than the two other published methods (64.5% better performance than the best literature method [1]). In row 6 of Table 3, total cost of SFCLs (installation and device costs) are

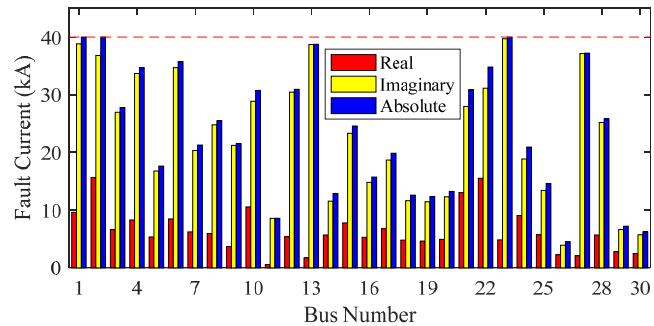

Fig. 6. *Bus fault currents of IEEE 30-bus transmission test system after SOP.*

Table 3. Comparison of the proposed SOP with previous methods in the IEEE 30-bus test system

Parameter	Method			
	Teng [8]	**Yu [1]**	**Proposed SOP by ABC**	**Proposed SOP by CABC**
Total excessive fault current before SOP (kA)	16.551	23.419	46.790	46.790
Number of SFCLs	5	3	4	3
Total SFCL size (Ω)	42.471	11.435	9.263	8.113
ASIPFC * (Ω/kA)	2.566	0.488	0.198	0.173
Total cost (M$)	27.11	9.14	9.15	7.46
Computation time (Sec)	1599	1377.92	434.21	255.63

*ASIPFC: Average SFCL impedance per fault current.

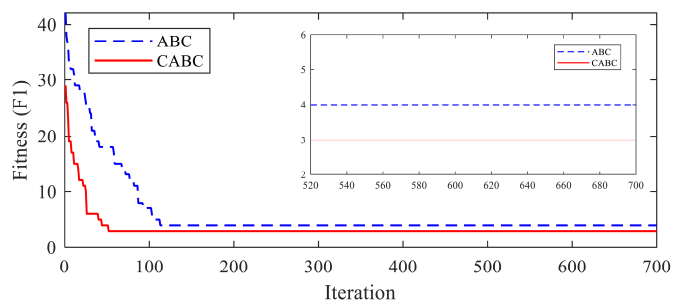

Fig. 7. *Convergence of F_1 in CABC and ABC algorithms for the IEEE 30-bus test system.*

reported considering cost details that are already given in Table 1 (we interpolate values from Table 1 for the nominal voltage 135 kV of the 30-bus test system). It is seen that the proposed SOP provides a more effective solution from the total cost point of view compared to the other methods. In the last row of Table 3, execution times of methods are given where the proposed SOP offers a faster approach. The CABC outperforms ABC in the table from the viewpoints of solution quality and execution time.

The convergence rate of the proposed SOP using the suggested CABC and basic ABC methods is depicted in Fig. 7. As seen, the CABC method achieves its solution at iteration 52, whereas the ABC method reaches its solution at iteration 118. The higher speed of CABC is due to the half-length of its solution vector (n-dimensional compared with $2n$-dimentional of ABC). A zoomed part of the last iterations is also shown in Fig.

7 for more convenience. The proposed CABC converges to a more optimal solution with $F_1 = 3$ compared to the basic ABC with $F_1 = 4$ implying a lower number of SFCLs obtained by CABC. This illustrates the enhanced exploration capability of the proposed CABC with respect to the basic ABC. The enhanced exploration is due to the CDV modeling that considers the mutual effects of real and imaginary parts of decision variables in the proposed CABC.

4.4. IEEE 31-bus distribution test system

The performance of the proposed SOP is also examined on the IEEE 31-bus 23kV distribution test system, the one-line diagram of which is shown in Fig. 8. This test system has one primary feeder and 6 lateral feeders as seen in Fig. 8. Fig. 9 depicts bus fault currents before placing SFCLs. Along each feeder, fault current level decreases from the beginning to the end of the feeder as shown in Fig. 9. There are four buses (1, 2, 3, and 29) with excessive fault currents in Fig. 9. As it can be observed, fault current real parts are more noticeable, unlike the transmission test system in the previous subsection, especially at end parts of feeders. In fact, at 18 end buses of feeders, the real part of fault currents dominates their imaginary counterpart unlike transmission systems. A vivid reason is that branches in distribution networks exhibit low X/R ratios. This feature also affects the optimal selection of resistive and inductive parts of SFCLs in the SOP. The proposed SOP locates just one resistive/inductive SFCL with the size of 0.0529 + j0.3180 Ω in series with the main transformer at bus 1 as shown in Fig. 8. By interpolating for 23 kV (the nominal voltage of the 31-bus test system) in Table 1, the total cost of this SFCL is obtained as \$0.6153M. Considering the essence of distribution networks, the reactance of this SFCL is about 6 times of its resistance. According to Fig. 9, the reason is that the real parts of fault currents are tangible on average, and thus, a resistive/inductive SFCL with higher reactance is more effective to alleviate excessive fault currents as confirmed by the sensitivity analysis presented in Subsection 2.3. Although the four excessive currents in Fig. 9 are mostly imaginary, a resistive/inductive SFCL best satisfies the SOP problem when all currents are taken into account. After placing the SFCL, fault currents are restricted to the 12.5 kA limit as shown in Fig. 10 (blue bars are the magnitudes of fault currents).

The value of the TIR index decreases from 1.63 in Fig. 9 to 1.56 in Fig. 10. This means that although the resistive/inductive SFCL reduces both real and imaginary fault currents, it declines the real fault currents more than the imaginary ones. This happens due to the higher sensitivity of real-part-dominated fault currents with respect to inductive SFCLs. Still, total imaginary current is higher due to $TIR > 1$. These TIR values are smaller than their counterparts in the IEEE 30-bus transmission test system because of a smaller difference between total real and imaginary fault currents in distribution systems. However, the rate of decrease of TIR after SFCL placement here is much lower than that of the transmission system.

The total excessive fault current in Fig. 9 is equal to 17.63 kA. Considering the size of SFCL as $|0.0529 + j0.3180|$ = 0.3224 Ω, the ASIPFC is calculated as 0.3324 Ω/17.63 kA = 0.019 Ω/kA. This means that we need 0.019 Ω of SFCL to decrease one kA of fault current. Compared with 0.173 Ω/kA ASIPFC of the proposed SOP in Table 3 for the transmission network, the ASIPFC of the distribution network is about 9 times smaller. That is, 1 Ω of SFCL reduces fault currents in the distribution network 9 times more effectively than the transmission network. This result further encourages distribution network planners to use SFCLs. In addition, as shown in Table 1, the unit price of 1 Ω distribution SFCL is lower than the unit price of 1 Ω transmission SFCL due to its lower voltage and insulation level. This more intensifies the usage of SFCLs in distribution networks from economic point of view.

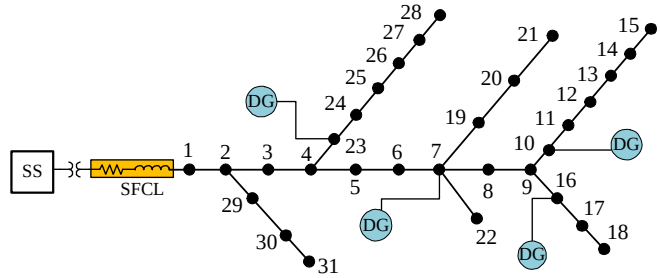

Fig. 8. *One-line diagram of the IEEE 31-bus distribution test system.*

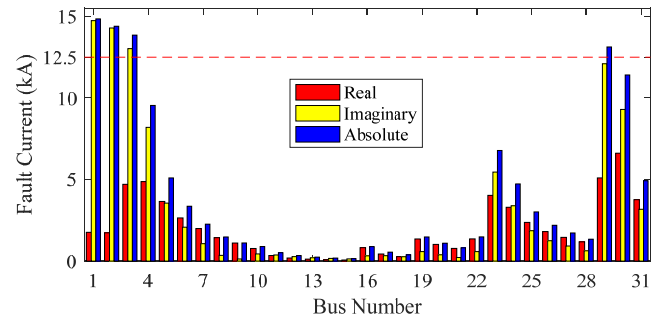

Fig. 9. *Bus fault currents of IEEE 31-bus distribution test system before SOP.*

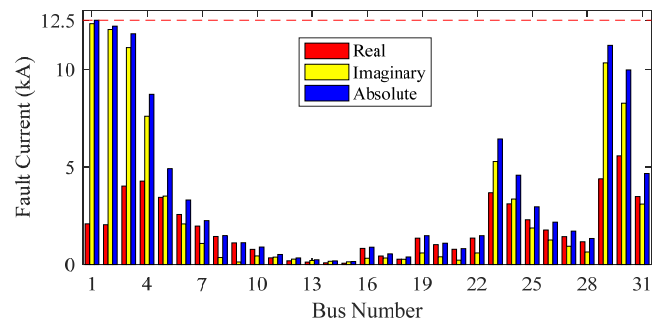

Fig. 10. *Bus fault currents of IEEE 31-bus distribution test system after SOP.*

5. Conclusions

In this paper, a SOP model is proposed to determine optimal number, types, and locations of SFCLs in power systems. By analyzing real and imaginary parts of fault currents, optimal resistive/inductive types of SFCLs can be located in both transmission and distribution networks considering their essence and

X/R ratios. Also, a new CABC method employing complex decision vector is proposed to solve the SOP problem. By examining the proposed SOP with CABC on the IEEE 30-bus transmission and 31-bus distribution networks, it is found that the optimal type of SFCL tends to decrease imaginary parts of fault currents. Also, it has been observed that in the transmission system mostly resistive SFCLs can better mitigate fault currents, whereas mostly inductive SFCLs are more appropriate for the distribution system. In addition, it has been shown that the proposed method outperforms the best literature SOP method by 64.5% better managing SFCL resources. In addition, SFCLs are more cost-effective in distribution systems than transmission systems when their capability in lowering one unit of fault currents is analyzed.

References

1 Yu, P., Venkatesh, B., Yazdani, A., Singh, B.N.: 'Optimal location and sizing of fault current limiters in mesh networks using iterative mixed integer nonlinear programming'*IEEE Trans. Power Syst.*, 2016, **31**, (6), pp. 4776–4783.

2 Wang, W., Jazebi, S., de Leon, F., Li, Z.: 'Looping radial distribution systems using superconducting fault current limiters: feasibility and economic analysis'*IEEE Trans. Power Syst.*, 2018, **33**, (3), pp. 2486–2495.

3 Alaraifi, S., El Moursi, M.S., Zeineldin, H.H.: 'Optimal allocation of HTS-FCL for power system security and stability enhancement'*IEEE Trans. Power Syst.*, 2013, **28**, (4), pp. 4701–4711.

4 Didier, G., Lévêque, J., Rezzoug, A.: 'A novel approach to determine the optimal location of SFCL in electric power grid to improve power system stability'*IEEE Trans. Power Syst.*, 2013, **28**, (2), pp. 978–984.

5 Angeli, G., Bocchi, M., Serri, L., Martini, L.: 'Short-circuit current limitation through 2G YBCO resistive-type SFCL devices: a model for technical and economic comparison with traditional air-core reactors'*IEEE Trans. Appl. Supercond.*, 2018, **28**, (4, Article no 5602505).

6 Yang, H.-T., Tang, W.-J., Lubicki, P.R.: 'Placement of fault current limiters in a power system through a two-stage optimization approach'*IEEE Trans. Power Syst.*, 2018, **33**, (1), pp. 131–140.

7 Zhu, J., Zhu, Y., Wei, D., *et al.*: 'Design and evaluation of a novel non-inductive unit for a high temperature superconducting fault current limiter (SFCL) with bias magnetic field'*IEEE Trans. Appl. Supercond.*, 2019, **29**, (5, Article no 5602404).

8 Teng, J.-H., Lu, C.-N.: 'Optimum fault current limiter placement with search space reduction technique'*IET Gener. Transm. Distrib.*, 2010, **4**, (4), pp. 485–494.

9 Ngoc, P.T., Singh, J.G.: 'Short circuit current level reduction in power system by optimal placement of fault current limiter'*Int. Trans. Electr. Energy Syst.*, 2017, **27**, (12), pp. 1–16.

10 Jo, H.C., Joo, S.K., Lee, K.: 'Optimal placement of superconducting fault current limiters (SFCLs) for protection of an electric power system with distributed generations (DGs)'*IEEE Trans. Appl. Supercond.*, 2013, **23**, (3, Article no 5600304).

11 Kim, Y., Jo, H.C., Joo, S.K.: 'Analysis of impacts of superconducting fault current limiter (SFCL) placement on distributed generation (DG) expansion'*IEEE Trans. Appl. Supercond.*, 2016, **26**, (4), pp. 1–5.

12 Jo, H.C., Joo, S.K.: 'Superconducting fault current limiter placement for power system protection using the minimax regret criterion'*IEEE Trans. Appl. Supercond.*, 2015, **25**, (3), pp. 1–5.

13 Khazali, A., Kalantar, M.: 'Optimal power flow considering fault current level constraints and fault current limiters'*Int. J. Electr. Power Energy Syst.*, 2014, **59**, pp. 204–213.

14 Mahmoudian, A., Niasati, M., Khanesar, M.A.: 'Multi objective optimal allocation of fault current limiters in power system'*Int. J. Electr. Power Energy Syst.*, 2017, **85**, pp. 1–11.

15 Elmitwally, A., Gouda, E., Eladawy, S.: 'Restoring recloser-fuse coordination by optimal fault current limiters planning in DG-integrated distribution systems'*Int. J. Electr. Power Energy Syst.*, 2016, **77**, pp. 9–18.

16 Karaboga, D., Akay, B.: 'A comparative study of artificial bee colony algorithm'*Appl. Math. Comput.*, 2009, **214**, (1), pp. 108–132.

17 Marzband, M., Azarinejadian, F., Savaghebi, M., Guerrero, J.M.: 'An optimal energy management system for islanded microgrids based on multiperiod artificial bee colony combined with Markov chain'*IEEE Syst. J.*, 2017, **11**, (3), pp. 1712–1722.

18 De, M., Goswami, S.K.: 'Optimal reactive power procurement with voltage stability consideration in deregulated power system'*IEEE Trans. Power Syst.*, 2014, **29**, (5), pp. 2078–2086.

19 Chen, L., Deng, Z., Xu, X.: 'Two-stage dynamic reactive power dispatch strategy in distribution network considering the reactive power regulation of distributed generations'*IEEE Trans. Power Syst.*, 2019, **34**, (2), pp. 1021–1032.

20 Grainger, J.J., Stevenson, W.D.: 'Power system analysis' (McGraw-Hill, 1994)

21 Rashidi, M., Farjah, E.: 'Lyapunov exponent-based optimal PMU placement approach with application to transient stability assessment'*IET Sci. Meas. Technol.*, 2016, **10**, (5), pp. 492–497.

22 Zitzler, E., Deb, K., Thiele, L.: 'Comparison of multiobjective evolutionary algorithms: empirical results.'*Evol. Comput.*, 2000, **8**, (2), pp. 173–195.

23 Zimmerman, R.D., Murillo-Sanchez, C.E., Thomas, R.J., Murillo-Sánchez, C.E., Thomas, R.J.: 'MATPOWER: Steady-state operations, planning, and analysis tools for power systems research and education'*IEEE Trans. Power Syst.*, 2011, **26**, (1), pp. 12–19.

24 Esmaili, M., Rajabi, M.: 'Optimal charging of plug-in electric vehicles observing power grid constraints'*IET Gener. Transm. Distrib.*, 2014, **8**, (4), pp. 583–590.

25 'SuperOx company', http://www.superox.ru/upload/FCL-full-information.pdf, accessed October 2019.